  Bull. Chem. Soc. Jpn., 59, 2053—2061 (1986)

Oxidation Reactions of a System Composed of Chloro(5,10,15,20-tetraphenylporphyrinato)cobalt(III) and Its π Cation Radical with Phenols

Masahiro KOHNO
JEOL Ltd., Akishima, Tokyo 196
(Received May 31, 1985)

The reactions of a system composed of chloro(5,10,15,20-tetraphenylporphyrinato)cobalt(III), [Co^{III}Cl(tpp)], and its π cation radical coordinating axially two chloride anions, [Co^{III}(tpp)$^{+\cdot}$]Cl_2, with several phenols were investigated by using ESR and optical absorption spectroscopy. The phenols were oxidized to phenoxyl radicals. The phenols investigated were classified into two groups after taking into account the differences in the reaction activities and their redox potentials, the phenols mainly reacting with [Co^{III}(tpp)$^{+\cdot}$]Cl_2 and those reacting with both [Co^{III}Cl(tpp)] and [Co^{III}(tpp)$^{+\cdot}$]Cl_2. The oxidation reactions of phenols with [Co^{III}(tpp)$^{+\cdot}$]Cl_2 were the second-order. A linear relationship between the rate constants of oxidation and the redox potentials of phenols was recognized. Active species in the reactions were determined to be composed of a chlorine radical which originates from axial ligands of [Co^{III}Cl(tpp)] and [Co^{III}(tpp)$^{+\cdot}$]Cl_2, and the porphyrin ligand of [Co^{III}(tpp)$^{+\cdot}$]Cl_2 itself. A possible mechanism for the oxidation reactions is proposed. Finally, the reaction scheme of cobalt porphyrin, ([Co^{II}(tpp)], [Co^{III}Cl(tpp)], and [Co^{III}(tpp)$^{+\cdot}$]Cl_2) with phenols is compared with oxidation reactions of phenols with horseradish peroxidase.

Peroxidase enzymes catalyze oxidation reactions of various kinds of substrates in the presence of hydrogen peroxide or substituted peroxides in biological systems. Because of the biologically important function of peroxidases, their structures, physicochemical properties, and reactivities have been extensively studied by many workers.[1] It has been known that horseradish peroxidase (HRP) takes on five different oxidation states: iron(II), iron(III), Compound II, Compound I, and Compound III, as characterized in the order of increasing oxidation states, and that Compound I is a π cation radical of iron(IV) porphyrin.[2] The π cation radicals of synthetic metalloporphyrins were prepared by chemical, electrochemical, or photochemical oxidation and their chemical natures have also been investigated.[3]

Previously, the electronic and molecular structures of chloro(5,10,15,20-tetraphenylporphyrinato)cobalt(III), [Co^{III}Cl(tpp)], were investigated by X-ray analyses, optical absorption, ^{1}H NMR, and ESR.[4-11] We have determined by ESR that [Co^{III}Cl(tpp)] is converted partially and reversibly into a paramagnetic species in chlorinated hydrocarbons by thermal and light activations.[4] This species was identified to be a π cation radical of chloro(5,10,15,20-tetraphenylporphyrinato)cobalt(III) with two axially coordinating chloride anions, [Co^{III}(tpp)$^{+\cdot}$]Cl_2.[5,6] The formation of this species in a [Co^{III}Cl(tpp)] solution was inevitable, even if a careful purification process of [Co^{III}Cl(tpp)] by column chromatography was carried out. It was recently clarified that [Co^{III}Cl(tpp)] in an aerated dichloromethane solution undergoes photooxidation to produce [Co^{III}(tpp)$^{+\cdot}$]Cl_2.[12] Hereafter, we treated the [Co^{III}Cl(tpp)] solution with a small amount of [Co^{III}(tpp)$^{+\cdot}$]Cl_2, denoted as [Co^{III}Cl(tpp)]-[Co^{III}(tpp)$^{+\cdot}$]Cl_2.

In the present study, we characterized the function of [Co^{III}Cl(tpp)]-[Co^{III}(tpp)$^{+\cdot}$]Cl_2. through an investigation of the reaction between these complexes and phenol derivatives by means of ESR and optical absorption spectroscopy and cyclic voltammetry. A possible reaction mechanism of these complexes with the phenols is proposed. Finally, the redox reaction scheme of the cobalt porphyrins with phenols is compared with that of horseradish peroxidase with phenols that is already known.

Experimental

Materials. Chloro(5,10,15,20-tetraphenylporphyrinato)-cobalt(III), [Co^{III}Cl(tpp)], was provided by Dr. K. Yamamoto of The Institute of Physical and Chemical Research.

2,6-Di-*t*-butyl-4-(3,5-di-*t*-butyl-4-oxocyclohexadienylidene)-methylphenol(PG), 2,4,6-tri-*t*-butylphenol(TBP), and 2,6-di-*t*-butyl-4-(3,5-di-*t*-butyl-4-oxo-2,5-cyclohexadienylideneamine)phenol(BIP) were prepared according to the literature.[13] 2,6-Di-*t*-butyl-4-methylphenol(BHT), 2,3-di-*t*-butyl-4-methoxyphenol(BHA), and α-tocopherol (vitamin E; VE), supplied from Wako Junyaku Co., were used without further purification.

A spin trapping reagent, nitrosodurene was supplied by Mr. N. Takahashi of Sumitomo Chemical Co. Ltd.

Preparation of Sample Solutions. Benzene was used as a solvent. [Co^{III}Cl(tpp)] was dissolved in 2×10^{-3} mol dm^{-3}. The solution of [Co^{III}Cl(tpp)] contained a small amount of the π cation radical, [Co^{III}(tpp)$^{+\cdot}$]Cl_2.[4,6] The concentration of [Co^{III}(tpp)$^{+\cdot}$]Cl_2 (2.7×10^{-5} mol dm^{-3}) was determined by comparing its ESR intensity with that of 2,2,6,6-tetramethyl-4-hydroxy-1-piperidyloxyl (98% radical) dissolved in benzene as a standard.

Concentrations of phenols (PG, BHT, TBP, BIP, and BHA) were adjusted to be 1.0×10^{-2} mol dm^{-3} and a 1% solution was employed for the VE system. All solutions were prepared just before use.

Measurements. The ESR and optical absorption spectra of the reaction mixtures were measured under deaerated

conditions in order to avoid any oxidation of the phenols. The ESR measurements were carried out with a JEOL FE-2XG spectrometer equipped with a Takeda Riken TR-5211 microwave frequency counter. The g-value and hyperfine coupling constant(hfcc) were calculated from the resonance frequency and the magnetic field. The optical absorption spectra were measured by a Hitachi 330 spectrophotometer using quartz cells with optical path lengths of 1 and 0.1 cm. Cyclic voltammograms were measured for the phenols (1.0×10^{-3} mol dm^{-3}) dissolved in dichloromethane with 0.1 mol dm^{-3} of tetrabutylammonium-tetrafluoroborate ($TBAF_4$). The cyclic voltammograms were recorded by a Yanagimoto P-1000H instrument at 25 °C at a scan rate of 100 mV s^{-1}. The redox potentials($E_{1/2}$) obtained from the cyclic voltammograms were checked by simultaneous polarographic measurement.

Time-dependent ESR spectra were measured using a rapid-detection system. To 0.2 cm^3 of the [$Co^{III}Cl$(tpp)]-[Co^{III}(tpp)$^{+\cdot}$]Cl_2 solution, which was bubbled by dry nitrogen gas, was added 0.2 cm^3 of the phenol solution (1×10^{-2} mol dm^{-3}).

Results

Reactions of [$Co^{III}Cl$(tpp)]-[Co^{III}(tpp)$^{+\cdot}$]Cl_2 with Phenols (PG, BHT, TBP, BIP, BHA, and VE). The ESR spectra measured before and after the addition of PG to the [$Co^{III}Cl$(tpp)]-[Co^{III}(tpp)$^{+\cdot}$]Cl_2 solution are shown in Fig. 1. The solid line represents the signal of [Co^{III}(tpp)$^{+\cdot}$]Cl_2.[5,6] Upon an addition of PG, the intensity of the signal decreased and a new ESR signal with doublet-triplet splittings appeared. The new signal(dotted line) was identified as a phenoxyl radical of PG (PG·) on the basis of ESR parameters; g=2.0043, a_{H1}=0.85 mT, a_{H2}=0.17 mT, which coincide with the literature values within the experimental errors.[14] Both the concentrations of the reduced [Co^{III}(tpp)$^{+\cdot}$]Cl_2 and oxidized PG were estimated to be 1.2×10^{-5} mol dm^{-3} under equilibrium states. The corresponding optical absorption spectra are shown in Fig. 2. An intense band at 406 nm (Soret band) and a moderate one at 540 nm (Q band) were determined to represent the characteristic absorption of [$Co^{III}Cl$(tpp)].[8] The spectrum obtained after an addition of PG showed no appreciable change in the region of the Soret and Q bands, except for a slight decrease in the absorption intensity in the region of 640—740 nm; this was interpreted to be due to a decrease in [Co^{III}(tpp)$^{+\cdot}$]Cl_2.[12] These spectral changes suggest that PG was oxidized to PG· and

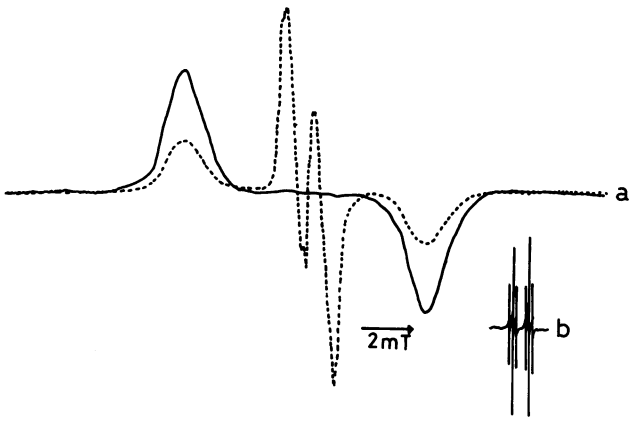

Fig. 1. a: ESR spectra measured before (——) and after (·····) addition of PG to [$Co^{III}Cl$(tpp)]-[Co^{III}(tpp)$^{+\cdot}$]Cl_2 in benzene at room temperature under degassed condition. b: The high resolution spectrum of center PG-phenoxyl radical.

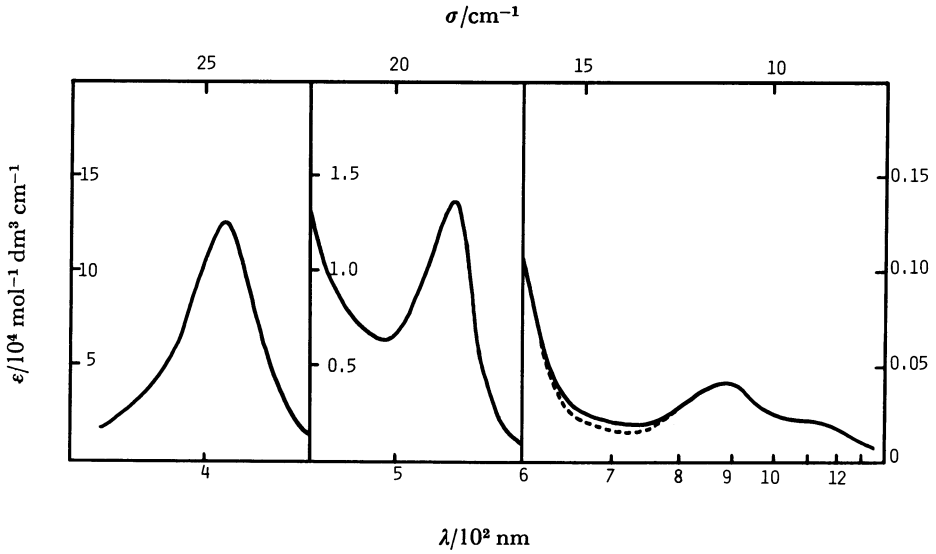

Fig. 2. Optical absorption spectra measured before (——) and after (·····) addition of PG to [$Co^{III}Cl$(tpp)]-[Co^{III}(tpp)$^{+\cdot}$]Cl_2 in benzene at room temperature under degassed condition.

$[Co^{III}(tpp)^{+\cdot}]Cl_2$ was reduced to $[Co^{III}Cl(tpp)]$, while the component $[Co^{III}Cl(tpp)]$ was unchanged.

In a reaction of $[Co^{III}Cl(tpp)]$-$[Co^{III}(tpp)^{+\cdot}]Cl_2$ with BHT or TBP, the phenol was oxidized to the corresponding phenoxyl radical (BHT· or TBP·),[15] and $[Co^{III}(tpp)^{+\cdot}]Cl_2$ was reduced to $[Co^{III}Cl(tpp)]$, as in the case of the PG system.

A reaction of $[Co^{III}Cl(tpp)]$-$[Co^{III}(tpp)^{+\cdot}]Cl_2$ with BIP also gave rise the formation of a phenoxyl radical (BIP·) (Fig. 3). The ESR parameters obtained from the spectrum are g=2.0036, a_N=0.21 mT, and a_H=0.104 mT. These values coincide with the reported values.[13] The concentrations of formed BIP· and the reduced $[Co^{III}(tpp)^{+\cdot}]Cl_2$ were 5.3×10^{-5} and 1.5×10^{-5} mol dm^{-3}, respectively. The concentration of formed BIP· was greater than that of reduced $[Co^{III}(tpp)^{+\cdot}]Cl_2$. This is different from the cases of the reaction with PG, BHT, or TBP. The optical spectrum of the reaction of $[Co^{III}Cl(tpp)]$-$[Co^{III}(tpp)^{+\cdot}]Cl_2$ with BIP showed that the Soret band of $[Co^{III}Cl(tpp)]$ shifts from 406 to 410 nm with an increase in the absorption intensity. The red shift of the Soret band can be attributed to a further reduction of $[Co^{III}Cl(tpp)]$ to $[Co^{II}(tpp)]$[16] in the BIP system.

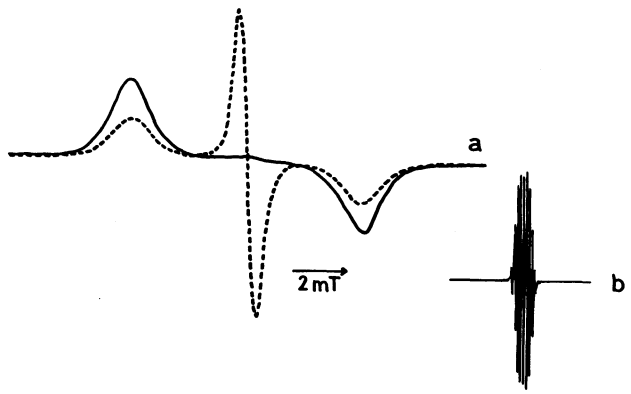

Fig. 3. a: ESR spectra measured before (——) and after (·····) addition of BIP to $[Co^{III}Cl(tpp)]$-$[Co^{III}(tpp)^{+\cdot}]Cl_2$ in benzene at room temperature under degassed condition. b: The high resolution spectrum of center BIP–phenoxyl radical.

When BHA and VE reacted with $[Co^{III}Cl(tpp)]$-$[Co^{III}(tpp)^{+\cdot}]Cl_2$, the ESR spectra of the reaction mixtures gave rise to new signals with a disappearance of the $[Co^{III}(tpp)^{+\cdot}]Cl_2$ signal. The new signals were assigned as BHA· and VE·, respectively.[17] The change in the optical absorption spectra of BHA is shown in Fig. 4. The absorption bands at 540 and 406 nm shifted to 530 and 410 nm, respectively, with an increase in absorption intensity. Furthermore, a weak band and a shoulder appeared at 1020 and 900 nm, respectively. The spectral change in the region of Q and the Soret bands indicates that a conversion of $[Co^{III}Cl(tpp)]$ to $[Co^{II}(tpp)]$ takes place in this system. The features of the ESR and optical absorption spectra show that BHA and VE react with both $[Co^{III}(tpp)^{+\cdot}]Cl_2$ and $[Co^{III}Cl(tpp)]$, as in the case of the BIP system. The appearance of new bands at the near-infrared region implies that isoporphyrin was formed. The absorption band is indeed complied with those of zinc- and iron-isoporphyrin.[18,19] For a comparison of such activities of phenols with their redox potentials, the oxidation potentials of the phenols under consideration were measured using cyclic voltammetry. The obtained potentials are listed in Table 1 with the ESR

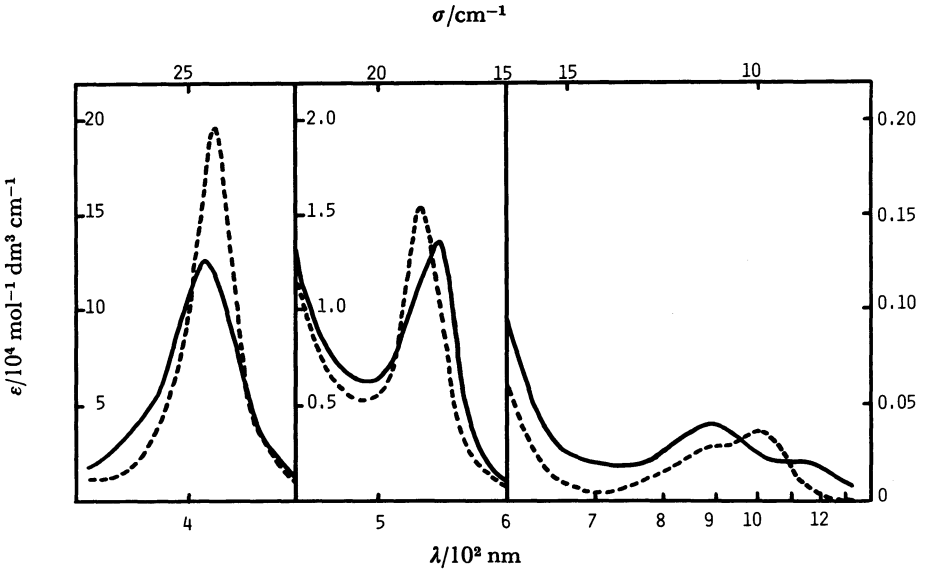

Fig. 4. Optical absorption spectra measured before (——) and after (·····) addition of BHA to $[Co^{III}Cl(tpp)]$-$[Co^{III}(tpp)^{+\cdot}]Cl_2$ in benzene at room teperature under degassed condition.

Table 1. ESR Parameters of Phenoxyl Radicals and Redox Potentials of Phenols[1)] and Rate Constants(k_f) of the Reactions between [Co^{III}(tpp)$^{+\cdot}$]Cl_2 and the Phenols

Phenoxyl radical	ESR parameter		$E_{1/2}$ CV_1(eV) vs. SCE	k_f $mol^{-1}\,s^{-1}$
	g-value	hfcc(mT)		
PG·	2.0043	a_{H1}: 0.85	1.66	4.5×10^2
		a_{H2}: 0.17		
TBP·	2.0043	unresoluble	1.16	3.6×10^3
BHT·	2.0045	a_H: 1.12	1.10	
BHA·	2.0045	a_H: 0.48	0.97	7.2×10^3
BIP·	2.0036	a_N: 0.21	0.89	
		a_H: 0.104		
VE·	2.0047	a_{H1}: 0.58	0.75	
		a_{H2}: 0.44		

1) PG: 2,6-di-*t*-butyl-4-(3,5-di-*t*-butyl-4-oxocyclohexadienylidene)methylphenol. TBP: 2,4,6-tri-*t*-butylphenol. BHT: 2,6-di-*t*-butyl-4-methylphenol. BHA: 2,3-di-*t*-butyl-4-methoxyphenol. BIP: 2,6-di-*t*-butyl-4-(3,5-di-*t*-butyl-4-oxo-2,5-cyclohexadienylideneamine)phenol. VE: α-tocopherol (vitamin E).

parameters of all the obtained phenoxyl radicals.

Kinetics of the Reaction between [Co^{III}(tpp)$^{+\cdot}$]Cl_2 and BHA, TBP, or PG. The time-dependent ESR spectra of mixed solutions of [Co^{III}(tpp)$^{+\cdot}$]Cl_2 (2.7×10^{-5} mol dm^{-3}) with BHA in a range from 1×10^{-2} to 6.25×10^{-4} mol dm^{-3} were measured at 30 °C by using the rapid detection system combined with the method described in the Experimental section. In Fig. 5, the concentration of [Co^{III}(tpp)$^{+\cdot}$]Cl_2 estimated from the ESR signal intensities is plotted against the reaction time (in second). It is seen that the decay rates of [Co^{III}(tpp)$^{+\cdot}$]Cl_2 depend on the concentration of BHA, even in its excess range, as will be discussed later. The rate constants (k_f) for TBP and PG were determined in a similar manner as that of BHA (1×10^{-2} mol dm^{-3}) at 30 °C as is also listed in Table. 1.

The temperature dependence of a reaction between [Co^{III}(tpp)$^{+\cdot}$]Cl_2 and PG (1×10^{-2} mol dm^{-3}) was examined in order to obtain information regarding their activities. Upon increasing the temperature from 30 to 80 °C, the concentration of [Co^{III}(tpp)$^{+\cdot}$]Cl_2 decreased rapidly along with a concomitant increase in that of PG·. The enthalpy changes for [Co^{III}(tpp)$^{+\cdot}$]Cl_2 and PG· were estimated to be −1.7 and 7.1 kJ mol^{-1}, respectively, from the exponential portion.

Detection of Active Species Derived from [Co^{III}Cl(tpp)]-[Co^{III}(tpp)$^{+\cdot}$]Cl_2. The active species was detected using a spin-trapping method.[20)] Among the various spin-trapping reagents tested for the detection, only nitrosodurene was effective to trap the

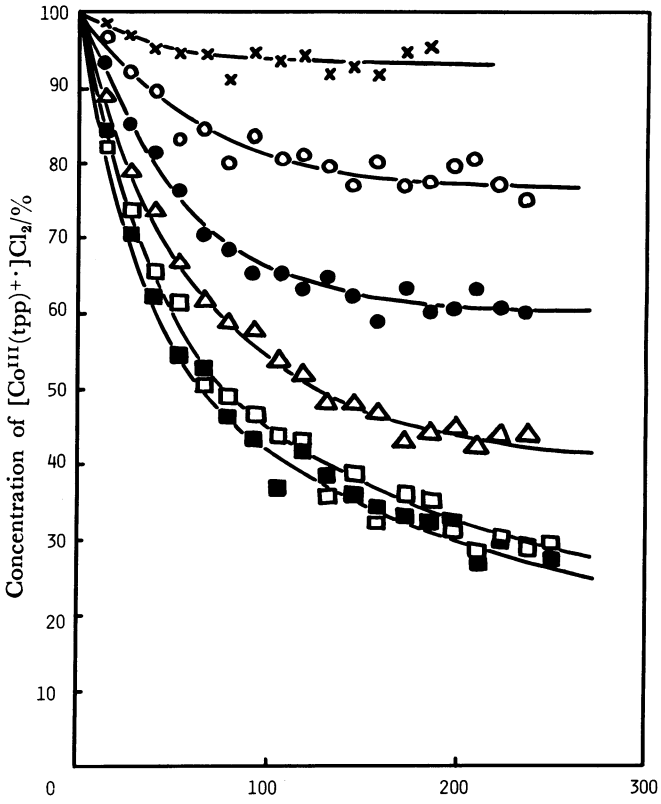

Fig. 5. Concentration decay of [Co^{III}(tpp)$^{+\cdot}$]Cl_2 in the reaction with BHA plotted against reaction time in second. Initial concentration of [Co^{III}(tpp)$^{+\cdot}$]Cl_2, 2.7×10^{-5} mol dm^{-3} and that of BHA, ■: 1.0×10^{-2}, □: 5.0×10^{-3}, △: 2.5×10^{-3}, ●: 1.25×10^{-3}, ○: 6.25×10^{-4} mol dm^{-3}, ×: blank.

species. To 1 cm^3 of the benzene solution of [Co^{III}Cl(tpp)]-[Co^{III}(tpp)$^{+\cdot}$]Cl_2, 3 mg of nitrosodurene was added under a degassed condition and the ESR spectrum was measured at room temperature.

The spin-trapping reaction is expressed as follows:

$$\text{R-N=O} + \text{X}\cdot \longrightarrow \text{R-N(X)-O}\cdot,$$

Scheme 1.

where X· is active species to be trapped. Figure 6 shows the ESR spectra of the spin adducts obtained by a reaction of [Co^{III}Cl(tpp)]-[Co^{III}(tpp)$^{+\cdot}$]Cl_2 with nitrosodurene. The spectra indicate the presence of two spin adducts (A and B). The following ESR parameters were obtained for A: one nitrogen (a_N=1.47 mT), one chlorine (a_{Cl}=0.284 mT), seven hydrogen (a_H=0.007 mT) nuclei, and for B; one nitrogen (a_N=1.47 mT) and seven hydrogen (a_H=0.007 mT) nuclei. From the ESR parameters, A was identified as a spin adduct of the nitrosodurene with a chlorine atom. The optical absorption spectrum which was measured after a reaction of [Co^{III}Cl(tpp)]-[Co^{III}(tpp)$^{+\cdot}$]Cl_2 with nitrosodurene in ben-

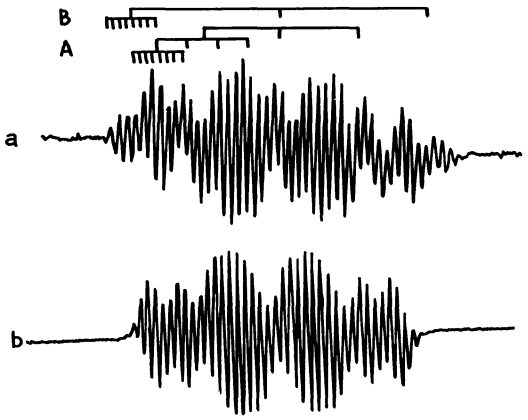

Fig. 6. ESR spectra of spin adducts (A and B) obtained from the reaction of nitrosodurene with [Co^{III}Cl(tpp)]–[Co^{III}(tpp)$^{+\cdot}$]Cl$_2$ in benzene at room temperature under degassed condition. Observed (a) and simulated for A (b) spectra.

zene at room temperature under a degassed condition showed the red shift of the Soret band, the blue shift of the Q band, and a decrease in the absorption intensity at around 600—700 nm. This spectral change was interpreted in terms of the formation of [Co^{II}(tpp)] from [Co^{III}Cl(tpp)] and [Co^{III}(tpp)$^{+\cdot}$]Cl$_2$. It is, thus, clear that the chlorine comes from axially coordinated chloride ligands in [Co^{III}(tpp)$^{+\cdot}$]Cl$_2$ and [Co^{III}Cl(tpp)]. This is the first case, to the auther's knowledge, that the active species in a reaction where metalloporphyrins participate has been directly detected. The second adduct B is probably a radical formed from nitrosodurene and a porphyrin ligand of [Co^{III}(tpp)$^{+\cdot}$]Cl$_2$.

Discussion

Based on the experiments described in the preceding section, phenols can be classified into two groups: group I (PG, TBP, and BHT) and group II (BHA, BIP, and VE). Phenols which belong to group II are more active than those of group I and are converted to phenoxyl radicals by both [Co^{III}(tpp)$^{+\cdot}$]Cl$_2$ and [Co^{III}Cl(tpp)], while phenols belonging to group I are oxidized only by [Co^{III}(tpp)$^{+\cdot}$]Cl$_2$. This difference in their activities can be explained in terms of the relative positions of the redox potentials of [Co^{II}(tpp)], [Co^{III}Cl(tpp)], [Co^{III}(tpp)$^{+\cdot}$]Cl$_2$, and phenols, as will be discussed in the following.

Regarding the oxidation process of the phenols, two oxidation mechanisms (1 and 2) have been proposed:[21]

$$\mathrm{POH} \xrightarrow[\mathrm{CV_1}]{-e} [\mathrm{POH}]^{+\cdot} \xrightarrow{-H^+} \mathrm{PO}\cdot \quad (1)$$

$$\mathrm{POH} \xrightarrow{-H^+} \mathrm{PO}^- \xrightarrow[\mathrm{CV_2}]{-e} \mathrm{PO}\cdot, \quad (2)$$

Scheme 2.

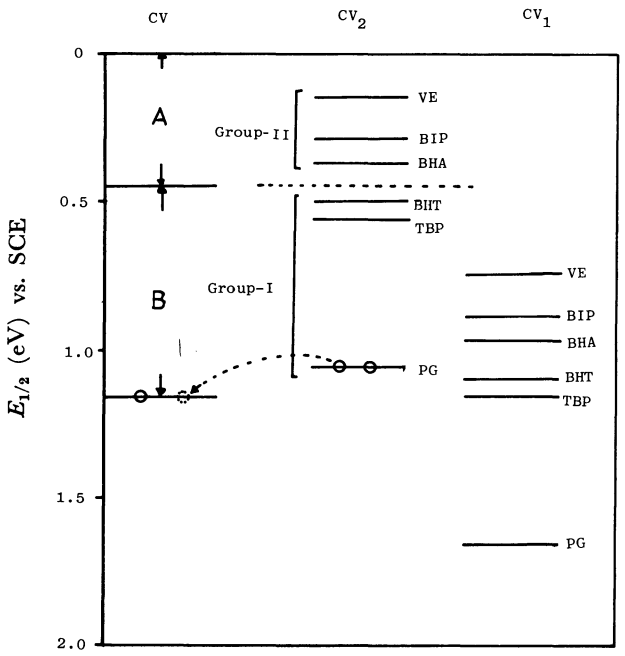

Fig. 7. Relative energy-level diagram of cobalt porphyrins and phenols. A and B represent half wave potential(CV) of [Co^{II}(tpp)]/[Co^{III}Cl(tpp)] and [Co^{III}Cl(tpp)]/[Co^{III}(tpp)$^{+\cdot}$]Cl$_2$, respectively. CV$_1$ represents half wave potential of phenols (POH)/phenol cation radicals ([POH]$^{+\cdot}$) and CV$_2$ phenolate anions (PO$^-$)/phenoxyl radicals (PO$\cdot$).

where phenols are abbreviated as POH. Process 1 means that first an electron is removed from phenol and then a proton is subtracted from the hydroxy group of the phenol to produce a phenoxyl radical.[22] In this process, the redox potential(CV$_1$) of POH/[POH]$^{+\cdot}$ obtained from a cyclic voltammogram should be the rate-determining factor. In process 2, first a proton is subtrated from the phenol, then, an electron transfer from phenolate anion follows. It has been reported[21] that the oxidation of 2,6-dimethylphenol(DMP) to diphenoquinone proceeds according to process 2 in the presence of a base(2,6-lutidine). A DMP–phenolate anion is formed through competition with the base. Such an ionic structure causes a decrease in the oxidation potential of the phenols. The redox potential (CV$_2$) of PO$^-$/PO$\cdot$ was estimated to be 0.6 eV lower than that of POH/[POH]$^{+\cdot}$(CV$_1$).[21]

In the present case, it is expected that the chloride anion of [Co^{III}Cl(tpp)] and/or [Co^{III}(tpp)$^{+\cdot}$]Cl$_2$ first forms an ion pair with the hydroxy proton of phenol and then process 2 proceeds predominantly. Here, we assume that in our case the oxidation potentials of phenolate anions formed are 0.6 eV lower than CV$_1$ of the precursor phenols. The energy-level scheme of phenols, [Co^{III}(tpp)$^{+\cdot}$]Cl$_2$, [Co^{III}Cl(tpp)], and [Co^{II}(tpp)] is given in Fig. 7 based on the cyclic voltammetries of these compounds. The CV$_2$ values of group I

phenols are lower than that of [$Co^{III}Cl$(tpp)]/[Co^{III}(tpp)$^{+\cdot}$]Cl_2[5] but higher than that of [Co^{II}(tpp)]/[$Co^{III}Cl$(tpp)], whereas the CV_2 values of group II phenols are higher than those of [$Co^{III}Cl$(tpp)]/[Co^{III}(tpp)$^{+\cdot}$]Cl_2 and [Co^{II}(tpp)]/[$Co^{III}Cl$(tpp)]. Consequently, the phenols of group I reduce only [Co^{III}(tpp)$^{+\cdot}$]Cl_2 but those of group II both [Co^{III}(tpp)$^{+\cdot}$]Cl_2 and [$Co^{III}Cl$(tpp)].

Possible Reaction Mechanism of [$Co^{III}Cl$(tpp)]-[Co^{III}(tpp)$^{+\cdot}$]Cl_2 with Phenols. When the concentrations of the phenols were of the same order as that of [Co^{III}(tpp)$^{+\cdot}$]Cl_2, the redox reaction did not proceeded. At concentrations 10^2 times higher than that of [Co^{III}(tpp)$^{+\cdot}$]Cl_2, however, the reaction process became spectroscopically detectable. A reaction of [$Co^{III}Cl$(tpp)]-[Co^{III}(tpp)$^{+\cdot}$]Cl_2 and PG showed that the amount of reduced [Co^{III}(tpp)$^{+\cdot}$]Cl_2 was equal to that of the generated PG phenoxyl radical. Furthermore, the redox reaction of [$Co^{III}Cl$(tpp)]-[Co^{III}(tpp)$^{+\cdot}$]Cl_2 by BHA proceeded depending on the concentration of BHA (Fig. 5). These facts give an indication that the reaction might be second order, as described by Eq. 1:

$$[Co^{III}(tpp)^{+\cdot}]Cl_2 + POH \rightarrow [Co^{III}Cl(tpp)] + PO^{\cdot} + HCl \quad (1)$$

In our reaction condition, however, Eq. 1 should be reduced by the pseudo-first-order. We have tried to plot $\ln a/(a-x)$ as a function of time for the reaction with BHA (shown in Fig. 5), where a and x are initial and reduced concentration of [Co^{III}(tpp)$^{+\cdot}$]Cl_2, respectively. As shown in Fig. 8, before 50 s reaction time, the functions show linear relationships, but after 50 s they deviate downward from the linear relationships, which means that the reaction does not follow the pseudo-first-order reaction rate. Next, we assumed that the phenolate anion activated in part from BHA reacts with the cation radical, as discussed in process 2. This means that in Eq. 1, PO^- instead of POH takes part in the reaction. Thus, we have tried to simulate the second-order decay rates k_f of [Co^{III}(tpp)$^{+\cdot}$]Cl_2;

$$k_f t = \frac{1}{(a-b)} \ln \frac{b(a-x)}{a(b-x')}, \quad (2)$$

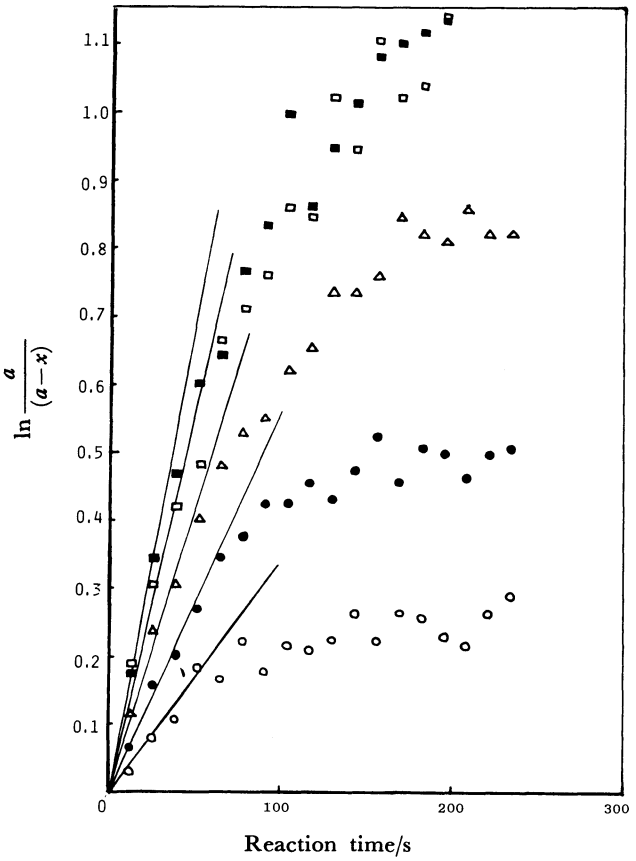

Fig. 8. In $a/(a-x)$ vs. time plot of the reaction between [Co^{III}(tpp)$^{+\cdot}$]Cl_2 and BHA, ■: 1.0×10^{-2}, □: 5.0×10^{-3}, △: 2.5×10^{-3}, ●: 1.25×10^{-3}, ○: 6.25×10^{-4} mol dm^{-3}.

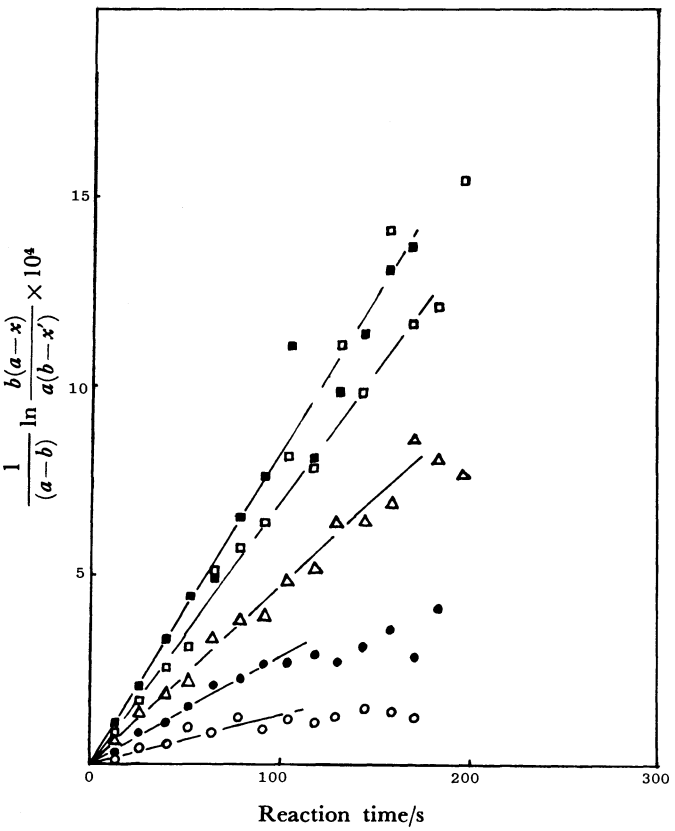

Fig. 9. $1/(a-b)\ln\{b(a-x)/a(a-x')\}$ vs. time plot of the reaction between [Co^{III}(tpp)$^{+\cdot}$]Cl_2 and BHA, ■: 1.0×10^{-2}, □: 5.0×10^{-3}, △: 2.5×10^{-3}, ●: 1.25×10^{-3}, ○: 6.25×10^{-4} mol dm^{-3}.

where a and x are the initial and reduced concentrations of $[Co^{III}(tpp)^{+\cdot}]Cl_2$ and b and x' are the initial and oxidized concentrations of the phenolate anion, respectively. Since b and x' are unknown, b has been substituted by trial values of 1.8 to 2.2×10^{-5} and x' is assumed to be equal to x. When the concentration of BHA anion is 2.1×10^{-5} mol dm^{-3}, the simulation accorded satisfactorily with the experimental data in whole concentration range of BHA (1.0×10^{-2}—6.25×10^{-4} mol dm^{-3}) as shown in Fig. 9. This means that the concentration of the phenolate anion is constant irrespective of the concentration change of phenol.

From these results, the reaction mechanism of $[Co^{III}(tpp)^{+\cdot}]Cl_2$ with the phenols may be written as follows:

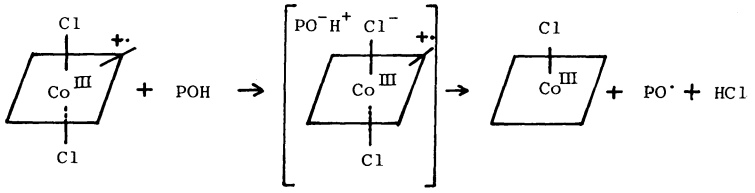

Scheme 3.

The chloride ligand of $[Co^{III}(tpp)^{+\cdot}]Cl_2$ attracts the hydroxy proton of phenol and a complex is formed, then, an electron transfer occurs from the phenolate anion to $[Co^{III}(tpp)^{+\cdot}]Cl_2$ in the complex to give a phenoxyl radical and $[Co^{III}Cl(tpp)]$. The fact that the reaction rates depend on the concentration of the phenols is related to the formation of the complex. In cases of reactions with group-II phenols, the chloride ligand of $[Co^{III}Cl(tpp)]$ also attracts its hydroxy protons. Thus, $[Co^{II}(tpp)]$ is formed through the formation of a similar complex:

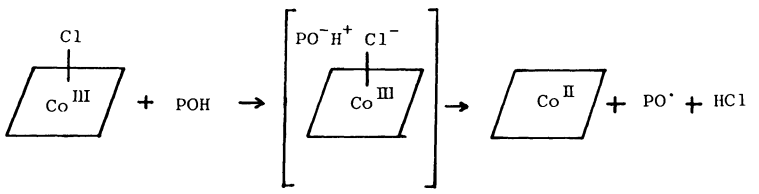

Scheme 4.

$[Co^{III}Cl(tpp)]$ and Horseradish Peroxidase(HRP). In the following we compare our results with the reaction of a typical enzyme HRP.[23] The function of $[Co^{III}Cl(tpp)]$–$[Co^{III}(tpp)^{+\cdot}]Cl_2$ and the enzymatic reaction of HRP are written in Schemes 5 and 6, respectively. The numbers in parentheses in these schemes represent the apparent oxidation states estimated on the basis of data from earlier work. $[Co^{III}(tpp)^{+\cdot}]Cl_2$ (+4) and Compound I (+5) of HRP are both π cation radicals and they perform two electron oxidation reactions. Here, we assume a correspondence of $[Co^{III}(tpp)^{+\cdot}]Cl_2$ with Compound I. Then, each of the other species in Scheme 5 can find a nice counterpart in Scheme 6. The change from $[Co^{III}(tpp)^{+\cdot}]Cl_2$ to $[Co^{III}Cl(tpp)]$ by a one-electron reduction corresponds to a reaction from Compound I to Compound II, and a change from $[Co^{III}Cl(tpp)]$ to $[Co^{II}(tpp)]$ to a reaction from Compound II to the native HRP–Fe(+3). This procedure enables us to write another correspondence: $[Co^{I}(tpp)]$ to HRP–Fe(+2), and $[Co^{III}(tpp)\text{-}O_2^{-\cdot}]$ to Compound III.[24] In our reaction system, the stable species is $[Co^{III}Cl(tpp)]$, corresponding to Compound II. The activity of $[Co^{III}Cl(tpp)]$ is considered to be due to its five-coordinate molecular structure[9] and the unique properties depending on the nature of the solvents[8] and the temperature.[10]

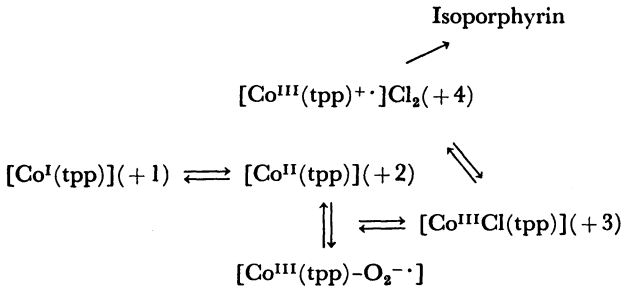

Scheme 5. Redox system of our case.

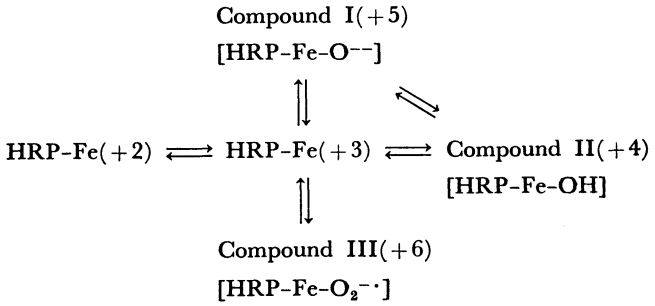

Scheme 6. Redox system of HRP.

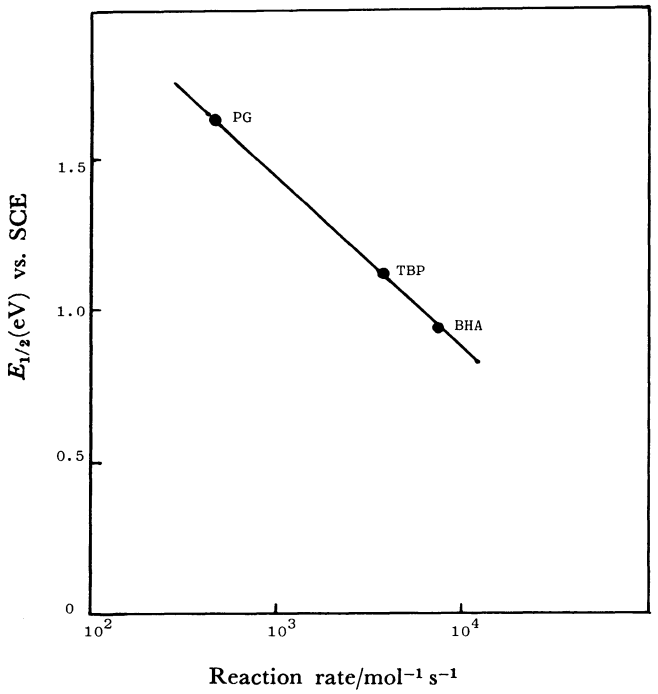

Fig. 10. Relation of reaction rates to redox potentials of phenols (PG, TBP, and BHA).

It should be noted that the active species conducting in our reactions was the chlorine radical, while the active species in the HRP system is considered to be an intermediate derived from H_2O_2.

Siga and Imaizumi[25] have reported that in the reactions of HRP-H_2O_2 and methemoglobin-H_2O_2, a phenoxyl radical formation from the phenols depends on their redox potentials. It has been found that the observed rate constants have a linear relationship with the redox potentials of the phenols. Therefore, the linear relationships shown in Fig. 10 indicate that the enzymatic reactions are correlated with the redox potentiels of the substrates. Furthermore, the concentration dependence of the rate constants shown in Fig. 9 has a similarity with that of the enzymatic reactions in which the concentration of the free radical formed depends upon that of the enzyme:[26] An excess amount of the substrates (more than 10^2 times that of the enzyme) is needed, and some activation mechanisms of the substrate are involved. Consequently, the good correspondence with [Co^{III}Cl(tpp)]-[Co^{III}(tpp)$^{+\cdot}$]Cl_2 and HRP suggests that knowledge of the molecular, electronic structure, and properties of [Co^{III}Cl(tpp)]-[Co^{III}(tpp)$^{+\cdot}$]-Cl_2 will give useful information for those of HRP.

The author wishes to express his deep gratitude to Prof. Hiroaki Ohya-Nishiguchi of Kyoto University and Dr. Kiyoko Yamamoto of The Institute of Physical and Chemical Research for their helpful discussions during the course of this study. The author is indebted to Mr. Akihiko Tajima of Ehime University for the measurements of cyclic voltammograms and useful discussions.

References

1) W. D. Hewson and L. P. Hager, "Peroxidases, Catalases, and Chloroperoxidase," in "The Porphyrins," ed by D. Dolphin, Academic Press. Inc., New York (1979), Vol. 7, p. 295 and other references cited therein.

2) a) D. Dolphin and R. H. Felton, *Acc. Chem. Res.*, **7**, 26 (1974); b) D. Dolphin, A. W. Addison, M. Cairns, R. K. Dinello, N. P. Farrell, B. R. James, D. R. Paulson, and C. Welborn, *Int. Quant. Chem.*, **16**, 311 (1979); c) J. E. Roberts, M. Hoffman, R. Rutter, and L. P. Hager, *J. Biol. Chem.*, **256**, 2118 (1981).

3) a) J. Fajer and M. S. Davis, "Electron Spin Resonance of Porphyrin π Cations and Anions," in "The Porphyrins," ed by D. Dolphin, Academic Press. Inc., New York (1979), Vol. 4, p. 197; b) M. A. Phillippi and H. M. Goff, *J. Am. Chem. Soc.*, **104**, 6062 (1982).

4) K. Yamamoto, M. Kohno, and H. Ohya-Nishiguchi, *Chem. Lett.*, **1981**, 255.

5) H. Ohya-Nishiguchi, M. Kohno, and K. Yamamoto, *Bull. Chem. Soc. Jpn.*, **54**, 1923 (1981).

6) M. Kohno, H. Ohya-Nishiguchi, K. Yamamoto, and T. Sakurai, *Bull. Chem. Soc. Jpn.*, **56**, 822 (1983).

7) M. Kohno, H. Ohya-Nishiguchi, K. Yamamoto, and T. Sakurai, *Bull. Chem. Soc. Jpn.*, **57**, 932 (1984).

8) K. Yamamoto, *Sci. Papers Inst. Phys. Chem. Res.*, **71**, 111 (1977).

9) T. Sakurai, K. Yamamoto, N. Naito, and N. Nakamoto, *Bull. Chem. Soc. Jpn.*, **49**, 3042 (1976).

10) K. Yamamoto, J. Uzawa, and T. Chijimatsu, *Chem. Lett.*, **1979**, 89.

11) K. Ichimori, H. Ohya-Nishiguchi, N. Hirota, and K. Yamamoto, *Bull. Chem. Soc. Jpn.*, **58**, 623 (1985).

12) K. Yamamoto, M. Hoshino, M. Kohno, and H. Ohya-Nishiguchi, *Bull. Chem. Soc. Jpn.*, **59**, 351 (1986).

13) G. M. Coppinger, *Tetrahedron*, **18**, 61 (1962).

14) a) K. Mukai, T. Mishina, K. Ishizu, and Y. Deguchi, *Bull. Chem. Soc. Jpn.*, **50**, 641 (1977); b) T. Yamamoto, M. Kohno, T. Miyamae, K. Mukai, and K. Ishizu, *Chem. Lett.*, **1972**, 681.

15) E. Mueller, K. Ley, K. Scheffer, and R. Mayer, *Chem. Ber.*, **91**, 2682 (1958).

16) G. D. Dorough, J. R. Miller, and F. M. Fuennekens, *J. Am. Chem. Soc.*, **73**, 4315 (1951).
17) a) K. Mukai, N. Tsuzuki, K. Ishizu, S. Ouchi, and K. Fukuzawa, *Chem. Phys. Lipids*, **29**, 129 (1981); b) K. Mukai, N. Tsuzuki, S. Ouchi, and K. Fukuzawa, *Chem. Phys. Lipids*, **30**, 337 (1982).
18) D. Dolphin, R. H. Felton, D. C. Borg, and J. Fajer, *J. Am. Chem. Soc.*, **92**, 743 (1970).
19) J. A. Guzinski and R. H. Felton, *J. Chem. Soc., Chem. Commun.*, **1973**, 715.
20) E. G. Janzen, *Acc. Chem. Res.*, **4**, 31 (1971).
21) K. Sasaki and A. Kunai, "Denkyoku-hanno Nyumon," Kagakudojin, Kyoto (1980), Chap. 5.
22) U. Svanholm, K. Bechgaard, and V. D. Parker, *J. Am. Chem. Soc.*, **96**, 2409 (1974).
23) I. Yamazaki and Y. Yokota, *Mol. Cell. Biochem.*, **2**, 39 (1973).
24) F. A. Walker, *J. Am. Chem. Soc.*, **92**, 4235 (1970).
25) T. Shiga and K. Imaizumi, *Arch. Biochem. Biophys.*, **167**, 469 (1975).
26) I. Yamazaki, H. S. Mason, and L. Piette, *J. Bio. Chem.*, **235**, 2444 (1959).